Al-Azhar Bulletin of Science

Volume 35 | Issue 2 Article 3

8-2024
Section: Earth science

Geomechanical Study of Rock Properties in the Kafr El-Sheikh Formation at Sapphire Field, West Delta Deep Marine, Egypt

Moustafa Mohamed Ahmed Attia
Halliburton World Wide Limited Company, Kuwait, Mostafa.attia16@gmail.com

Ali El-Sayed Farag
Halliburton World Wide limited Company, UAE

Mahmoud Y. Zein El-Din
Geology Department, Faculty of Science, Al Azhar University, Cairo, Egypt

How to Cite This Article

Attia, Moustafa Mohamed Ahmed; Farag, Ali El-Sayed; and Zein El-Din, Mahmoud Y. (2024) "Geomechanical Study of Rock Properties in the Kafr El-Sheikh Formation at Sapphire Field, West Delta Deep Marine, Egypt," *Al-Azhar Bulletin of Science*: Vol. 35: Iss. 2, Article 3.
DOI: https://doi.org/10.58675/2636-3305.1674

ORIGINAL ARTICLE - EARTH SCIENCE

Geomechanical Study of Rock Properties in the Kafr El-Sheikh Formation at Sapphire Field, West Delta Deep Marine, Egypt

Moustafa Mohamed Ahmed Attia [a,*], Ali El-Sayed Farag [b], Mahmoud Youssry Zein El-Din [c]

[a] Halliburton World Wide Limited Company, Kuwait
[b] Halliburton World Wide Limited Company, UAE
[c] Department of Geology, Faculty of Science, Al-Azhar University, Cairo, Egypt

Abstract

Numerous challenges were encountered during the drilling operations conducted at the Sapphire oilfield. Instances of stuck pipe, wellbore instability, breakouts, and washouts have been documented in many wells within this field, resulting in unproductive time and additional expenditures. To mitigate these challenges, it is important to conduct a one-dimensional geomechanical model to get a viable resolution. This entails the creation of three primary in situ stress profiles and the assessment of mechanical characteristics of the geological formations. The primary focus of this investigation was to ascertain the mechanical characteristics of the rock. Therefore, this work offers great input while building a comprehensive one-dimensional mechanical earth model in a set of wells situated in the Sapphire field, which is situated inside the West Delta Deep Marine region. Nevertheless, the understanding of these values is impeded by the lack of extensive rock mechanics testing data, encompassing both mechanical and elastic characteristics. The rock's mechanical properties were calculated using empirical equations due to the lack of core sample data, which required using wireline data instead. The unconfined compressive strength in the present study was calculated based on Young's modulus correlation, initially developed by Dick Plumb, and it showed a good correlation with the well events. Using the rocks' geomechanical properties helps explain the formation's fracability and shows how likely it is to collapse. The occurrence of wellbore instability issues is more probable in shale intervals compared with other geological formations. These results revealed that the shale beds are most likely to fail as Poisson's ratio and Young's modulus of shale are all rather high, but they have a lower friction angle. Hence, to prevent instability issues, the proposed wells must be meticulously engineered.

Keywords: Elastic properties, Kafr El-Sheikh formation, Rock strength, West delta deep marine Egypt

1. Introduction

When a rock undergoes deformation, it is possible to extract several constitutive laws that may be used to characterize this particular behavior. The correlation between stress and strain is a key principle in the field of rock mechanics. In the drilling process, borehole deformation is closely related to in-situ stress and rock mechanical properties. Therefore, it should be beneficial if such deformation data can be used to determine in situ stresses and/or rock mechanical properties [1]. The characteristics of rocks may be characterized by the analysis of their behavior under elastic and inelastic deformations. The assessment of geomechanical properties, such as elastic properties and rock strength, has considerable significance in the context of wellbore-stability investigations. Furthermore, they play a crucial role in ascertaining the regional stress conditions, which is vital information for the investigation of wellbore stability. The most effective approach for acquiring data on the attributes of formations is to use

Received 7 January 2024; revised 14 March 2024; accepted 17 March 2024.
Available online 17 May 2024

* Corresponding author.
E-mail address: mostafa.attia16@gmail.com (M.M.A. Attia).

https://doi.org/10.58675/2636-3305.1674

a mix of laboratory experiments that integrate geomechanics, acoustic velocities, permeability, and porosity. These experiments may be used to calibrate the wireline and/or LWD log data. Nevertheless, because of the unavailability of cores for our investigation, every parameter was derived using wireline data and appropriate empirical relationships [2]. Rock characteristics may be classified into two distinct groups: elastic properties and rock strength. The three main factors that determine the elastic characteristics of a composite material, like sedimentary rock, are the proportions of its constituent parts, the elastic properties of each part individually, and the geometric arrangement of each part [3].

The elastic characteristics of rocks include four distinct moduli, namely Poisson's ratio, shear, Young's modulus, and bulk modulus. Rock strength encompasses several characteristics, such as unconfined compressive strength (UCS), internal friction angle, and tensile strength. The rock strength parameters include the qualities of shear strength and tensile strength. Shear strength is a quantification of the shear stress that arises as a consequence of failure caused by substantial compressive stresses. Tensile failure occurs as a consequence of tensile stresses that exert a pulling force, leading to the separation of the rock. The shear strength parameters include three key factors: the coefficient of internal friction, cohesion, and UCS [4].

This work aims to calculate the rock mechanical parameters to assist in establishing a one-dimensional mechanical earth model, which will lead us to determine a safe mud window and prevent wellbore stability problems. The sonic model was used to compute the dynamic moduli from the sonic log (shear and compressional) and bulk density log to estimate the dynamic shear modulus (Gdyn) and bulk modulus (Kdyn). The UCS profile was estimated based on static Young's modulus correlations. The profile of the internal friction angle was estimated using a map of gamma-ray correlation to the internal friction angle with a linear relationship. Finally, the profile of tensile strength was determined based on UCS. The estimated profile of the mechanical properties of the rock was not calibrated due to a lack of core data. However, the absence of core data in this study resulted in uncertainty, but the results matched the collapse events that took place during the drilling of the studied wells. The principal keys, Sapphire-Da and Sapphire-Db, are used in this writing.

2. Geological overview

The Sapphire field lies about 90 km (56 mi) from the coast of Alexandria, on the northwestern edge of the Nile Delta. It lies within the West Delta Deep Marine concession. It lies at the cross of Lat 32° 01′ 43.192′ N and long 30° 21′ 10.707′ E (Fig. 1). The major structures within the West Delta Deep Marine concession are the northeast-southwest trending Rosetta fault, the east northeast-west southwest trending Nile Delta offshore anticline and rotated

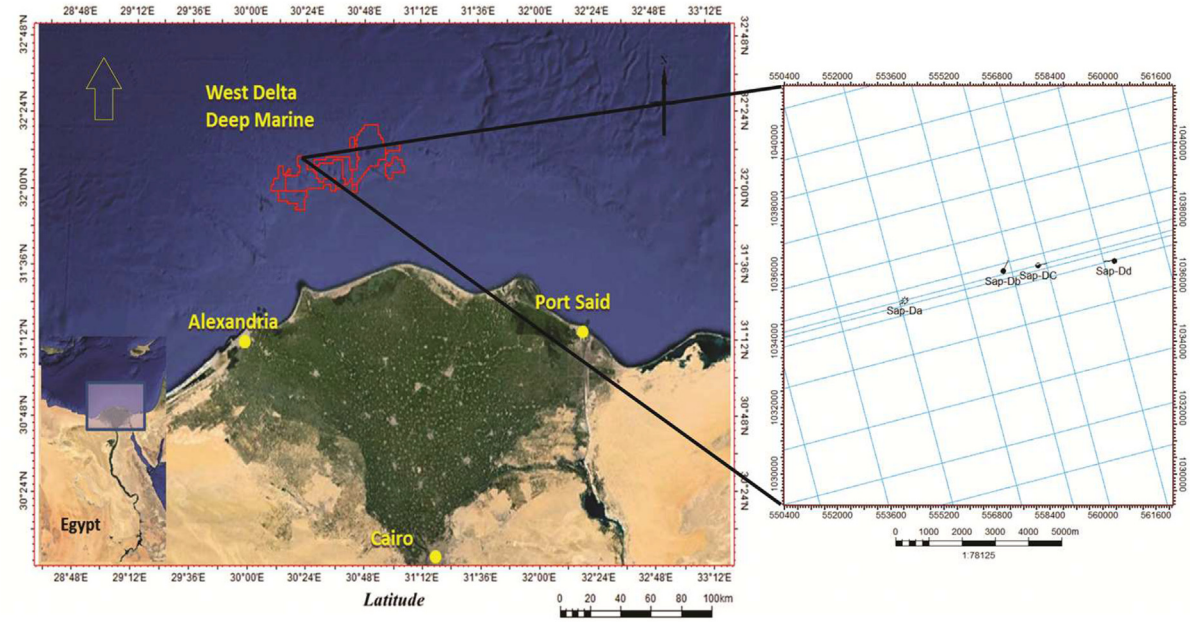

Fig. 1. Adapted from Google Maps, this map shows e the West Delta Deep Marine concession boundaries including Sapphire Field with the provided wells from EGPC. Located ~90 km from the Alexandria coast.

fault blocks in the Northeast [5]. When it comes to clastic wedges, the Nile Delta system is by far the biggest in the Mediterranean. Since the late Miocene epoch, it has been formed by the deposition of clastic sediments from the Nile River. The Nile Delta is made up of two distinct clastic delta systems, one inactive (Jurassic–Miocene) and one active (Pliocene–Holocene), as a result of ongoing tectonic activity since the Cenozoic epoch [6]. During the Pliocene transgressive phase, the shale of the Kafr El-Sheikh formation was deposited and followed by a regression that deposited sand in the top part of the formation as well as in the overlying (El Wastani) sequence. The Kafr El-Sheikh Formation overlies the Abu Madi formation with a gentle erosion surface. It extends laterally over the whole area of the delta with constant characteristics. The upper limit of the Kafr El-Sheikh formation can be easily identified because the large sand layers of the El Wastani formation begin to appear. The sedimentary environment is the outer shelf, or perhaps also the slope, in the northernmost areas. The field's Pliocene sandstones (the Kafr El-Sheikh formation) yielded a gas discovery. The reservoir is made up of a series of sandstones, claystones, and siltstones that gradually increase in thickness (Fig. 2).

3. Materials and methods

In the field of geomechanical analysis, the evaluation of rocks' mechanical properties is crucial. Elastic properties such as Poisson's ratio (v), shear modulus (G), bulk modulus (K), and Young's modulus (E) are essential mechanical features of rocks. Meanwhile, rock strength properties such as internal friction angle (FANG), UCS, and tensile strength are also important.

All of the strata in the study region exhibit intrinsic diversity in strength and formability, as seen by the continuous profile of these properties. The data used in this research include conventional borehole logs, including neutron, density, GR, sonic, and caliper. After loading the data and performing log QC, the computation of mechanical properties was calculated using several empirical equations using the IP 2018 software.

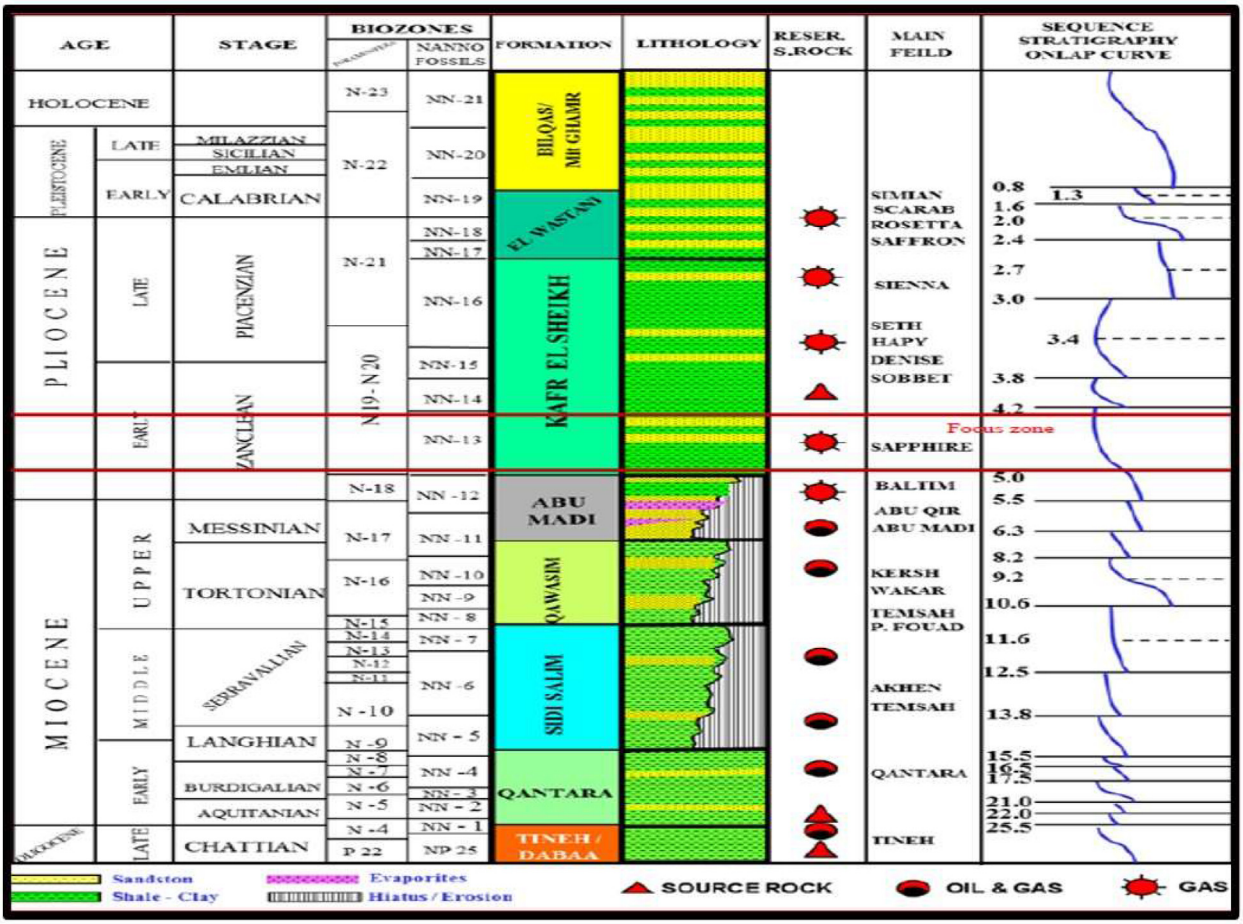

Fig. 2. Stratigraphic sequence and hydrocarbon system of the Nile delta, including Sapphire Field [7].

The workflow is shown in Fig. 3.

3.1. Elastic properties

Young's modulus, Poisson's ratio, shear modulus, and bulk modulus are the four types of elastic moduli that may be measured on rocks. High-frequency impulse (dynamic testing) is used to assess bulk density and acoustic travel time. The data used in this research include conventional borehole logs, including neutron, density, GR, sonic, and caliper. After loading the data and performing log QC, the computation of mechanical properties was calculated using several empirical equations using the IP 2018 software.

3.2. Young's modulus (E)

The stiffness degree of the rock is called Young's modulus [3]. The relationship between stress (σ) and strain (Ɛ) is determined by Hooke's law, which describes a linear correlation. The equation proposed by Hooke is given as follows: [8]. The formula used in well logging for the determination of *E*:

$$E = \frac{\left(\frac{pb}{(DTS)^2}\right)\left(3DTS^2 - 4DTC^2\right)}{DTS^2 - DTC^2} \times 1.35 \times \left(10^{30}\right) \quad (1)$$

where ***pb*** is the density, and ΔTS and ΔTC are shear and compressional sonic, respectively [9].

The dynamic E is defined as the stress-to-strain ratio. The stress is dimensionless. It can be determined using the following equation:

$$Edyn = \frac{(9Gdyn) \times Kdyn}{Gdyn + 3Kdyn} \quad (2)$$

Gdyn is the shear modulus and Kdyn is the bulk modulus. They are measured in Mps units. The static Young's modulus of the behavior of the sample is often influenced by the prevailing stress conditions, together with the frequency and amplitude of the applied strain during measurement. The literature has several associations that have been

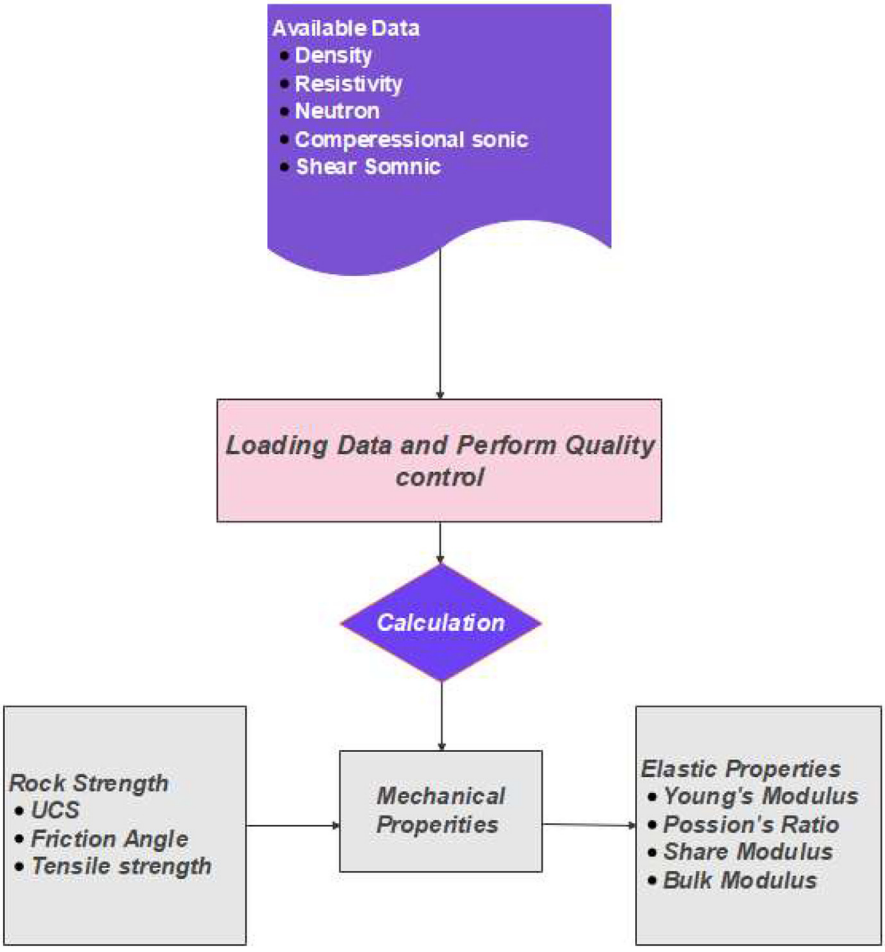

Fig. 3. Flow chart showing the research steps.

reported [10]. The symbol Esta is used to denote the static Young's modulus, whereas Edyn is used to indicate the dynamic Young's modulus [11].

There are several methods for computing static Young's modulus:

(1) Modified Morales correlation.

Grain-supported rocks like sandstone can benefit greatly from the present method, which derives the static Young's modulus from the dynamic Young's modulus and the total porosity. John Fuller correlation: the current approach uses a mechanism that derives the static Young's modulus by using the dynamic Young's modulus. The correlation analysis is conducted using a dataset consisting of sandstone samples collected from the North Sea. The observed values for UCS of sand, based on a sample size of around 20, mostly fall between the range of 2000 and 10 000 psi. The correlation was established using triaxial core measurements of the YME formation under confinement of 1 MPa, together with similar DSI log points obtained from the same well. This methodology may be used for sandstone as well as shale.

(2) Plumb Bradford correlation.

Plumb Bradford used Edyn to compute an Esta from this equation:

$$\text{Esta} = 0.0018 \times (\text{Edyn})\,2.7 \tag{3}$$

The calibration technique in this research was complicated by the unavailability of core test data on the static Young's modulus in this particular location. In this research, we used the Plumb–Bradford correlation method.

One possibility is that this method provides the highest degree of accuracy available for determining the static Young's modulus. Its strength lies in its alignment and compatibility with dynamic information. When compared with more conventional methods, these display fewer distortions and produce more reliable outcomes. Predictions of porosity were made using the connection between the static and dynamic Young's moduli. The existence of a very porous formation is indicated by a considerable disparity between the static and dynamic Young's moduli. However, if the variation is small, that may indicate that the formation has been highly consolidated. The findings demonstrated novel associations between Edyn and Esta by an examination of the interval encompassing well Sapphire-Da. These correlations exhibited a strong link (Fig. 4).

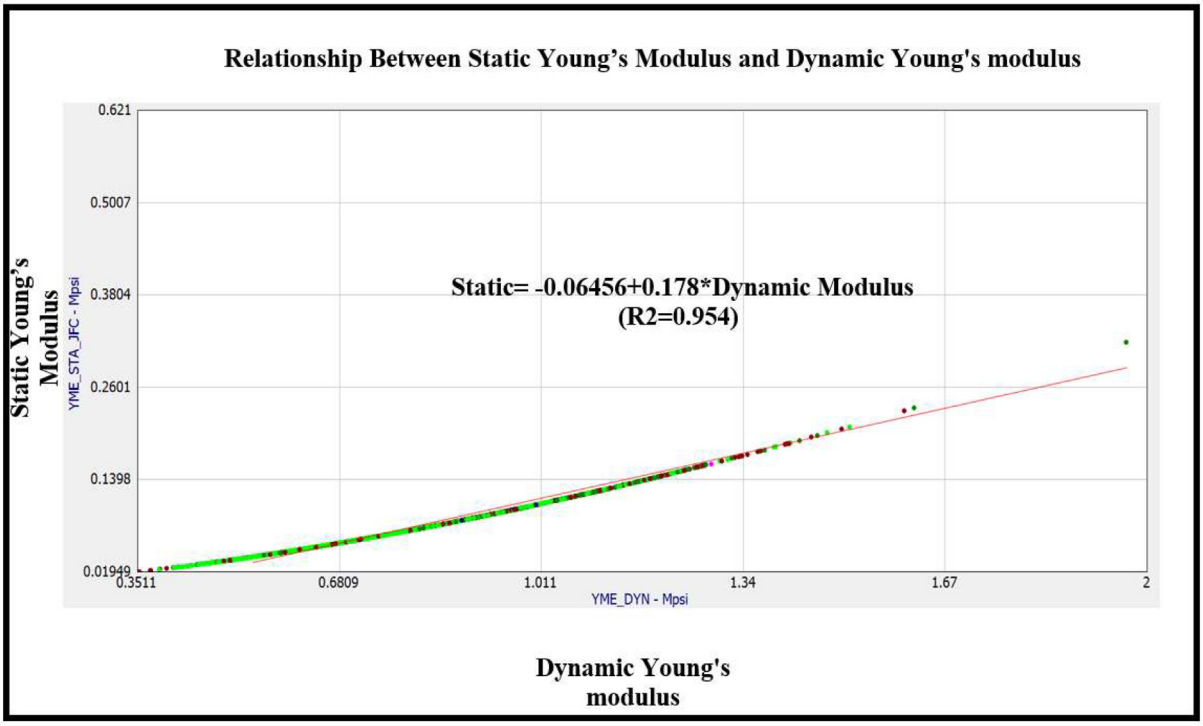

Fig. 4. The relationship between static and dynamic Young's modulus may be distinguished by using GR values as a discriminating factor.

3.2.1. Shear modulus

The shear modulus (G) quantifies the extent to which a rock undergoes deformation when subjected to shear stress. The quantity being referred to is the ratio of shear stress (τ) to shear strain (γ), as shown by citation [12].

The equation can be expressed as:

$$G = \tau / \gamma \tag{4}$$

The shear modulus attribute is indicative of a material's ability to withstand shearing deformation. According to Zoback [13], when a material exhibits high resistance to shearing, it is capable of efficiently transmitting shear energy at a rapid rate. Shear forces cannot be sustained in fluids that do not permit the transmission of shear waves. Consequently, it can be seen that the materials possess shear moduli that approach zero [13]. The shear modulus is seen when a force is applied parallel to a surface. This force has the potential to induce sliding between objects or to cause the deformation of initially rectangular objects into parallelograms. It can be calculated by

$$G_{dyn} = (13474.45)\left(\frac{pb}{DTS^2}\right) \tag{5}$$

or

$$G_{dyn} = \left(\frac{pb}{DTS^2}\right) * 1.34 * 10^{30} \tag{6}$$

where Gdyn is the shear modulus, ΔTS the shear sonic, and *pb* is the bulk density of the formation (g/cm^3) [12].

This feature of significant importance provides advanced insight into the resistance of a material to shear deformation. When the material exhibits high stiffness in response to shearing forces, it facilitates the rapid transmission of shear energy. The application of shear stress is necessary to induce deformation in a material, as quantified by the tangent of the resulting angle of deformation. Strain being a dimensionless quantity, it follows that the shear modulus will be expressed in units of Pascal. The static shear modulus can be calculated from the equation

$$G\,sta = \frac{Esta}{2(1 + Vsta)} \tag{7}$$

where Gdyn is the shear modulus and the vsta is the Poisson's ratio.

3.2.2. Bulk modulus

The bulk modulus (K) refers to the measure of stiffness exhibited by a material when subjected to volumetric compression. The idea being explored relates to the connection between stress (σ) and the volumetric strain [13]:

$$K = \sigma / (\Delta v / v) \tag{8}$$

Equation (8) represents the relationship between the coefficient of thermal conductivity (K), the thermal conductivity (σ), and the relative change in velocity (Δv/v). The symbol Δv represents the volume after deformation, whereas v represents the starting volume. When the rock has a substantial size, it demonstrates little compression even when subjected to significant loads, indicating a high degree of stiffness. When the size of an object is tiny, it exhibits a high susceptibility to compression, allowing even a relatively low pressure to induce significant deformation in the material. According to Zoback [14], gases have a much lower bulk modulus compared with solids and liquids. K refers to the dynamic bulk, and Ksta refers to the static bulk modulus.

They are calculated from the following equations:

$$K = 13474.45\rho_b\left[\frac{1}{(DTC)^2}\right] - \frac{4}{3}G \tag{9}$$

$$Ksta = \frac{Esta}{3(1 - 2vsta)} \tag{10}$$

3.2.3. Poisson's ratio

It measures how much axial shortening a rock experiences during its expansion. Following Fig. 5, the value represents the ratio of horizontal strain to vertical strain [13]:

$$\nu = \varepsilon h \,/\, \varepsilon v \tag{11}$$

In the above equation, ν represents the dimensionless Poisson's ratio, whereas εh and εv denote the horizontal and vertical strains, respectively. The consideration of Poisson's ratio is of significant importance in drilling operations, as it influences the behavior of plastic rocks, which tend to compress around the wellbore. To avoid well collapse, it is essential to use a larger mud weight when dealing with rocks that possess a higher Poisson ratio.

Static Poisson's ratio '*v* sta': the static Poisson's ratio could be calculated from the dynamic one as in this equation:

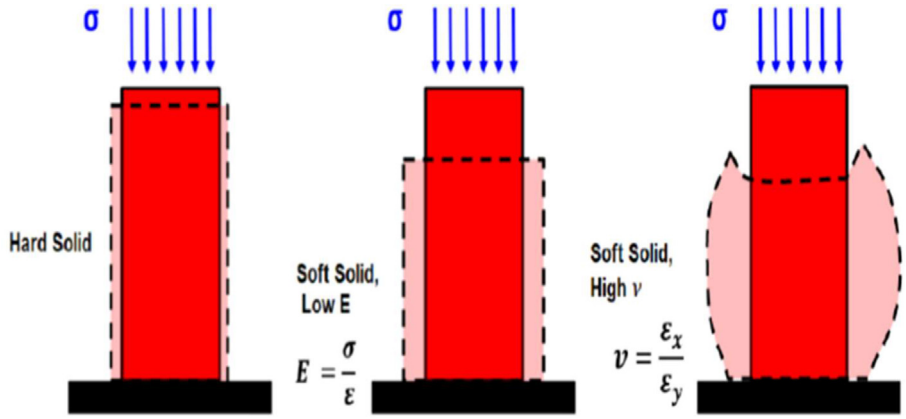

Fig. 5. Analysis of deformed solids representing Young's modulus and Poisson's ratio [15].

$$\nu sta = \nu dyn * \nu - multiplier \quad (12)$$

where νsta is the static Poisson's ratio; νdynamic is the dynamic Poisson's ratio; and the unit of the ν multiplier is unitless. When ν-multiplier is set to its default value of 1, the static Poisson ratio is identical to the dynamic Poisson's ratio.

Dynamic Poisson's ratio '*v*dyn': according to Zoback [14], with the values of compressional slowness (VP) and shear velocity (VS) provided in this study, a mathematical method is introduced that may be used to determine the *v dyn*. This formula may alternatively be represented by using sonic as follows:

$$v = \frac{\frac{1}{2}\left(\frac{Vp}{Vs}\right)^2 - 1}{\left(\frac{Vp}{Vs}\right)^2 - 1} \text{ Or } v = \frac{\frac{1}{2}\left(\frac{DTS}{DTC}\right)^2 - 1}{\left(\frac{DTS}{DTC}\right)^2 - 1} \quad (13)$$

As per Zoback [14], it can be computed using Bulk and Shear modulus as follows:

$$v\,dyn = \frac{3K\,dyn - 2G\,dyn}{6K\,dyn + 2G\,dyn} \quad (14)$$

3.3. Rock strength properties

The rock strength parameters include the qualities of shear strength and tensile strength. Shear strength is a quantification of the shear stress that leads to failure as a consequence of excessive compressive pressures. Tensile failure occurs as a consequence of tensile stresses that exert forces in opposite directions, causing the rock to undergo separation. The shear strength parameters include the coefficient of internal friction, tensile strength, and UCS [4].

3.3.1. Friction angle (Φ)

The friction angle (Φ) refers to the inclination of a slope relative to the horizontal at which an object positioned on the slope would begin sliding. The parameter quantifies the rock's capacity to resist shear stress. The friction angle for clay-supported materials typically ranges from 20 to 25°, whereas for grain-supported materials, it ranges from 35 to 40°. The size and shape of the grains exposed on the fracture surface are related to the friction angle of the rock material, as reported by Schlumberger's media outlets. Because of this, the friction angle is often lower in rocks with a fine-grained texture and a high mica content and higher in rocks with a coarse-grained structure. Table 1 presents a comprehensive overview of the customary ranges of friction angles observed in various kinds of rock. The most effective means of determining the friction angle is through the performance of a uniaxial compressive strength test. When core measurements are not accessible, the friction angle may be determined by referring to the empirical correlations (Table 2).

In this study, a GR log and linear connections were used to find the internal friction angle. This

Table 1. Angles of friction for common rock types [16].

Rock class	Friction angle range (deg.)	Typical rock type
Low friction	20–27	Schists (high mica content), shale, and marl
Medium friction	27–34	Sandstone, siltstone, chalk, and slate
High friction	34–40	Basalt, granite, limestone and conglomerate

Table 2. Models with equation used to calculate friction angel [17].

Model and reference	Equation	Remarks
FANG-Dt (Lal, 1999)	$\theta = \sin^{-1}\left(\left(\frac{304878}{Dt} - 1000\right)/\left(\frac{304878}{Dt} + 1000\right)\right)$	Shales
FANG-M (McPhee *et al.*, 2000)	$\theta = 1.0691 \times 10^{-6}M + 28.51$	Sandstone, Bongkot Field, Gulf of Thailand.
FANG-V $V_{\text{clay}} - 1$ (Plumb, 1994)	$\theta = 26.5 - 37.4(1 - \phi - V_{clay}) + 62.1(1 - \phi - V_{clay})^2$	Both sandstones and shales
FANG- $V_{\text{clay}} - 2$	$\theta = 20.5 + 15(1 - V_{clay})$	Sandstones
FANG- $\phi 1$ (Weingarten and Perkins, 1995)	$\theta = 57.8 - 105\phi$	Sandstones
FANG- $\phi 2$ (Perkins and Wngarten, 1988)	$\theta = 58 - 135\phi$	Weak sandstones
FANG- ρ_b	$\tan\theta = 0.1\rho_b^{2.85}$	Sandstones

technology converts gamma photons into angles of refraction. A cutoff condition has been implemented. The GR 120 API value is converted to a friction angle of 20°. The default translation of the GR 40 unit is thought to be comparable to the friction angel 35° unit.

$$\phi = \tan - 1(78 - 0.4\,\text{GR60}) \tag{15}$$

3.3.2. Tensile strength

The determination of the lowest and greatest horizontal stresses may be achieved by considering the breaking strength of rock as a significant contributing element. Given that bit penetration disrupts an otherwise complete rock state, it is common practice to presume that the tensile strength of unconsolidated formations is zero. This will not be the case in highly compacted and robust formations that are subjected to significant in situ pressures.

A brittle failure occurs when a material breaks extremely suddenly in the lab without undergoing any plastic deformation. Other materials, including most metals, are more ductile and may undergo plastic deformation and even necking before they break. Laboratory core measurements are the gold standard for determining tensile strength. Lacking core data analysis such as this study, it is common practice to estimate all facies' tensile strength to be between 10 and 12% of the UCS. This approach might be faulty as tensile strength is influenced by a wide variety of variables, including lithology type, compaction degree, lamination orientation, and the presence of microscopic cracks. The mechanism used here makes it easy to derive tensile strength from UCS:

$$\text{TSTR} = \text{K} * \text{UCS} \tag{16}$$

where K is the facies and zone-based factor, default: 0.1. In this study, the tensile strength has been used as a function of UCS.

3.3.3. Unconfined compressive strength

UCS and internal friction coefficient are frequent indicators of rock strength. To develop a secure mud weight window, the UCS is a crucial parameter for forecasting shear failure. The UCS and internal friction coefficient (μ) are considered to be the primary rock strength characteristics of utmost significance. Laboratory core measurements under uniaxial loading stress circumstances provide the most reliable estimate of UCS. It is possible that UCS correlations calculated in one area would not hold in another. It is important to implement rigorous validation and calibration procedures using laboratory measurements. As core samples were not available for this study, the UCS values were calculated using well-known empirical correlations from the literature that are related to lithology and petrophysical parameters. The suggested artificial intelligence methodology exhibits potential suitability for the estimation of strength characteristics [18].

The present investigation uses Young's modulus correlation initially developed by Dick Plumb in 1994 and subsequently updated in 2002 to estimate UCS, as demonstrated in the provided equation:

$$\text{UCS} = 4.242\,\text{Esta} \tag{17}$$

4. Results

The determination of the dynamic elastic properties is conducted by the use of the acoustic model, which is based on assumptions of a formation that exhibits homogeneity, isotropy, and elasticity. The dynamic bulk modulus 'K' and dynamic shear modulus 'Gdyn' were initially determined by the use of compression and shear sonic logs, in conjunction with density logs, by applying equations (6) and (9). Following that, the values for the dynamic Young's modulus 'Edyn' and dynamic Poisson's ratio '*v*dyn' were determined using equations (2) and (4) respectively.

The association between the static Poisson's ratio 'vsta' was established by equation (12). The constant value, referred to as the PR multiplier, was established at 1.0 in the absence of any laboratory testing protocols. The values collected exhibited comparatively elevated values inside shale zones (ranging from 0.41 to 0.48), while sandstone intervals had lower values (ranging from 0.24 to 0.31).

The results indicated that shale rocks exhibited greater values in comparison to sandstone, whereas siltstone had intermediate values between sandstone and shale. The estimation of the static Young's modulus, referred to as 'Esta' was determined by the use of the Plumb-Bradford technique, utilizing the dynamic Young's modulus. The Young's modulus values for shaly beds range from 0.55 to 0.80 million pounds per square inch (Mpsi), whereas for sandy intervals, the range is from 0.7 to 1.5 Mpsi. Figures 6 and 7 depict the elastic characteristics of two examined wells inside the Sapphire Field. Poisson's ratio of shaly formations is greater in comparison to formations with a lower shale content.

Determination of the friction angle was conducted by the examination of the gamma-ray log. The sandstone formations displayed elevated values, ranging from 30° to 35°, whereas the shale layers showed lower values ranging from 24° to 28°. The estimation of UCS was conducted using equation (17).

Determination of tensile strength (TSTR) may be inferred from the UCS using equation (15). The UCS estimates for sandstone exhibited relatively low values ranging from 500 to 700 psi, which may be attributed to its friable nature as a kind of sandy rock. The pressure inside shaly intervals has a somewhat elevated range, often ranging from 800 to 1300 psi. A whole set of findings are presented in Figs. 6 and 7.

Correlation between total porosity and internal friction angle exhibits an inverse relationship. This correlation is supported by the plum clay. Volume and porosity correlation is depicted in Fig. 8.

5. Discussion

The rock's mechanical properties were calculated using empirical equations due to the lack of core sample data, which required using wireline data instead. A high Poisson ratio is caused by the fact that shale formations have different axial and transverse strain deformation rates. This is because they contain clay. This assertion applies to every one of the static and dynamic Poisson's ratio values associated with shaly formations. The sonic velocity in shale is comparatively lower than that in more resilient rock formations, mostly attributable to the distinctive composition of shale. Consequently, there was an increase in compressional transit time and an even greater increase in shear transit time,

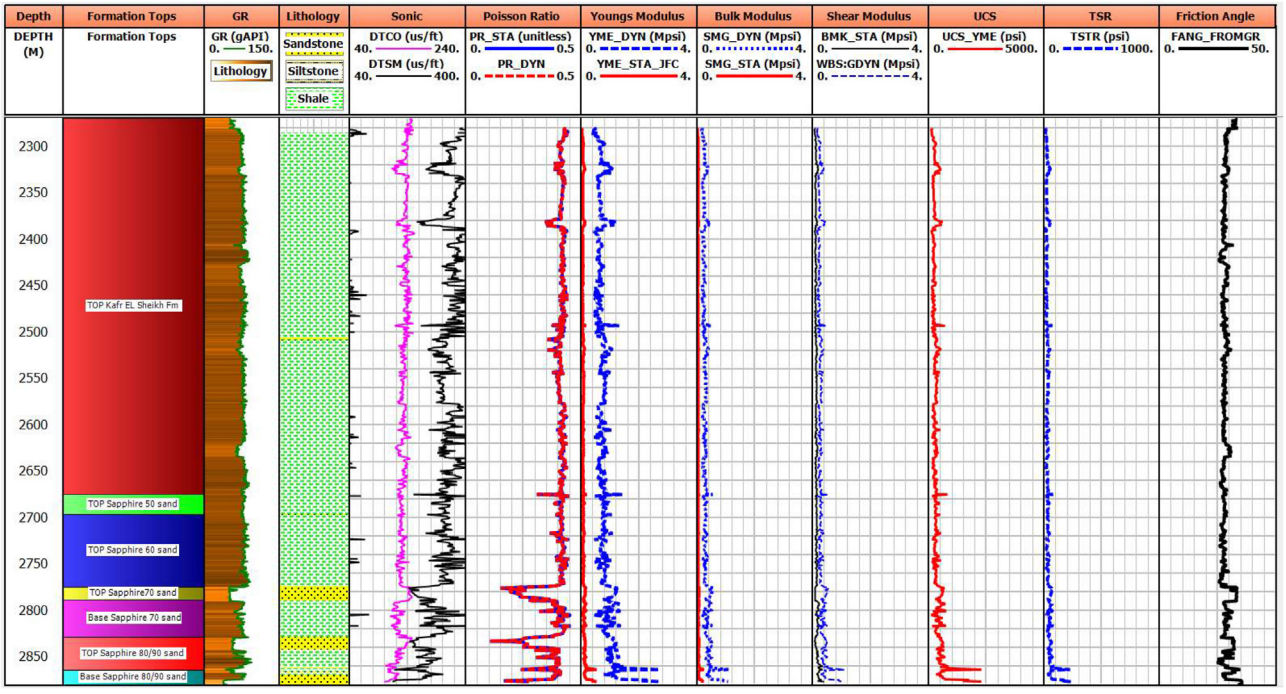

Fig. 6. Elastic properties result in well Sapphire-Da.

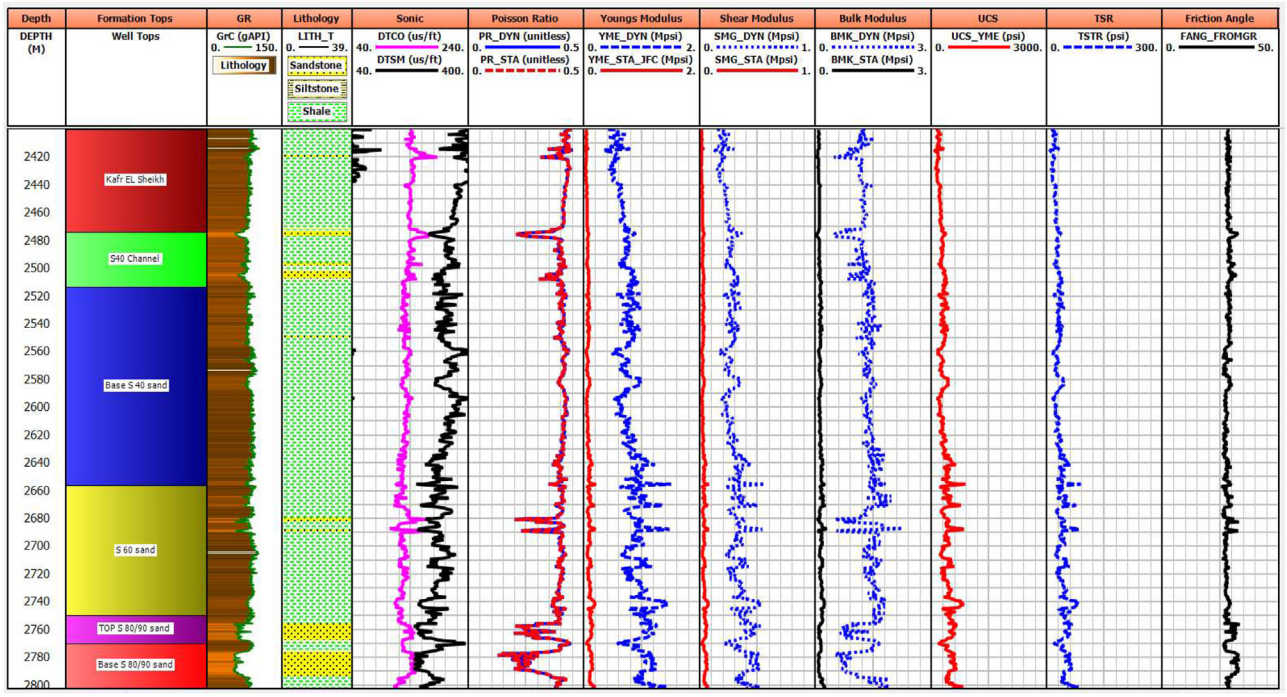

Fig. 7. Elastic properties result in well Sapphire-Db.

both of which are essential components for calculating Poisson's ratio. Because of this, it is clear that wellbore instability problems are more likely to happen in shale intervals than in other units as Poisson's ratio is higher and Young's modulus is lower.

The obtained findings of rock strength validate the previously reported available data on elastic

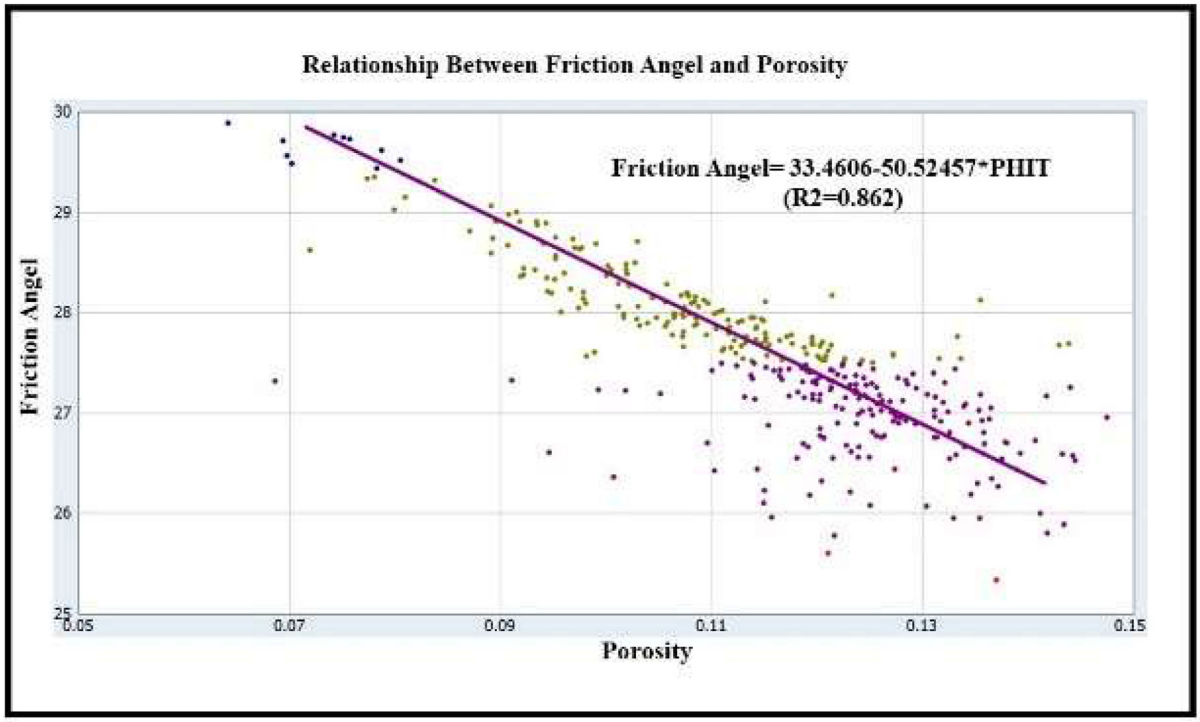

Fig. 8. Relationship between friction angle and total porosity.

characteristics, which indicate that the shale beds are prone to failure as they significantly elevate Poisson's ratio, have a relatively diminished Young's modulus, and have a comparatively reduced friction angle. Hence, it is essential to meticulously construct the proposed wells to mitigate any issues related to instability. Using regression analysis, we were able to study the relationship between elastic moduli and shear waves, using an equation to predict shear waves from compressional waves using the available data in the absence of shear waves.

5.1. Correlation between elastic moduli and shear wave

For this study, we used the least-squares regression method to examine the elastic moduli calculated and S-wave velocity. Figure 9 depicts a linear connection between shear modulus, Young's modulus, and S-wave velocity. Correlation coefficients (R^2) and the regression equations used to reach those conclusions are also displayed in Fig. 9. Straight lines were the best-fitting lines in every single situation. Elastic moduli tend to get larger as P-wave velocities rise. With an R^2 value better than 0.90, the correlations are statistically significant. Insightful linearity between elastic moduli and S-wave velocity in Sapphire sediments is indicated by the strong correlation.

5.2. Shear-wave forecasting based on compressional wave information

The present study examines the empirical correlations used for the estimation of shear-wave velocity. The findings from the study indicate that there are notable discrepancies in shear-wave velocities, which may be attributed to factors such as material composition, its state (which includes compaction and toughness), and structural loading circumstances. It was decided that laboratory measurement was required to deal with the difficulty of determining the shear-wave velocity or getting an approximation of it. The acquired results from laboratory-based velocity estimates on rock samples are not very typical as they only apply to a very small volume of rocks. It is important to take into account the in situ circumstances of tension, fluid content, and other relevant factors in rock samples. Therefore, measurements conducted on samples in a laboratory setting will exhibit substantial variations compared with the values seen in their original environment. The environmental reliance on stress is notably evident in the acoustic qualities of rock. Therefore, it is essential to devise a technique for calculating shear-wave velocity while simultaneously mitigating the financial burden associated with its acquisition. Within this particular framework, several empirical associations have been proposed through the use of regression analysis to approximate shear-wave velocity. This estimation is achieved by employing easily accessible compressional wave velocity or other petrophysical data. By utilizing a set of independent variables, also known as predictor variables, regression analysis is a typical statistical method for investigating relationships between an important dependent variable and a set of independent ones [20]. Regression analysis may be categorized into two main types: linear regression and nonlinear regression. In this research, an equation was formulated to establish the correlation between compressional and shear velocity, as elucidated in the study region. To mitigate any potential inconsistencies in subsequent analyses, a plot of shear velocity versus compressional velocity was generated using exponential regression. A robust positive association ($R^2 = 0.94$) was detected throughout the inquiry of the Sapphire-Db Well (Fig. 10). The following equation can be used in the present study to examine the empirical correlations used for the estimation of shear-wave velocity. The findings from the study indicate that there are notable discrepancies in shear-wave velocities, which may be attributed to factors such as material composition, its state (which includes compaction and toughness), and structural loading circumstances. It was decided that laboratory measurement was required to deal with the difficulty of determining the shear-wave velocity or getting an approximation of it. The acquired results from laboratory-based velocity estimates on rock samples are not very typical as they only apply to a very small volume of rocks. It is important to take into account the in situ circumstances of tension, fluid content, and other relevant factors in rock samples. Therefore, measurements conducted on samples in a laboratory setting will exhibit substantial variations compared with the values seen in their original environment. The environmental reliance on stress is notably evident in the acoustic qualities of rock. Therefore, it is essential to devise a technique for calculating shear-wave velocity while simultaneously mitigating the financial burden associated with its acquisition. Within this particular framework, several empirical associations have been proposed through the utilization of regression analysis to approximate shear-wave velocity. This estimation is achieved by using easily accessible compressional wave velocity or other petrophysical data. By using a set of independent

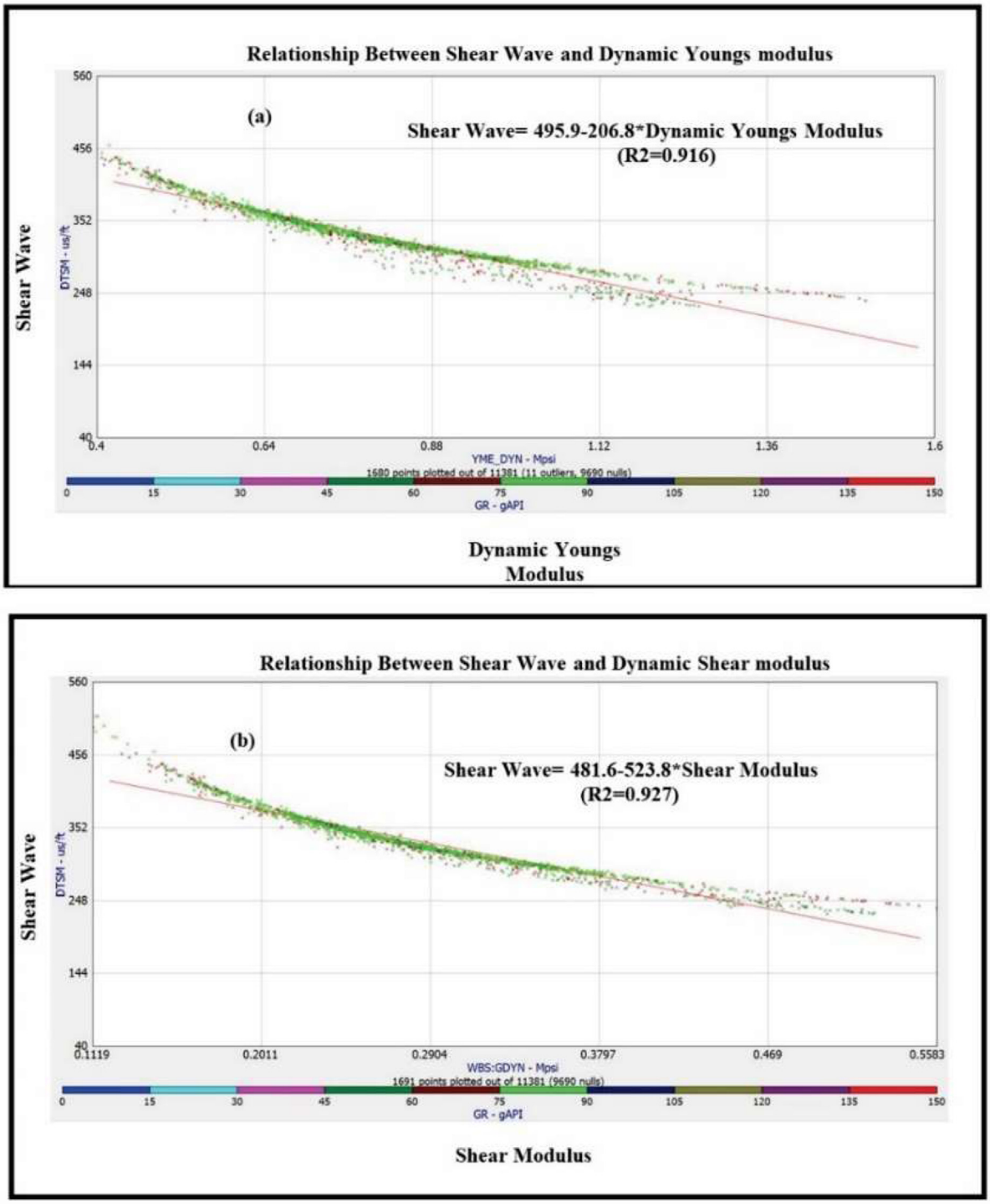

Fig. 9. The relationship between elastic moduli and S-wave velocity.

variables, also known as predictor variables, regression analysis is a typical statistical method for investigating relationships between an important dependent variable and a set of independent ones [19]. Regression analysis may be categorized into two main types: linear regression and nonlinear regression. In this research, an equation was formulated to establish the correlation between compressional and shear velocity, as elucidated in the study region. To mitigate any potential inconsistencies in subsequent analyses, a plot of shear velocity versus compressional velocity was generated using exponential regression. A robust positive association ($R^2 = 0.94$) was detected throughout the

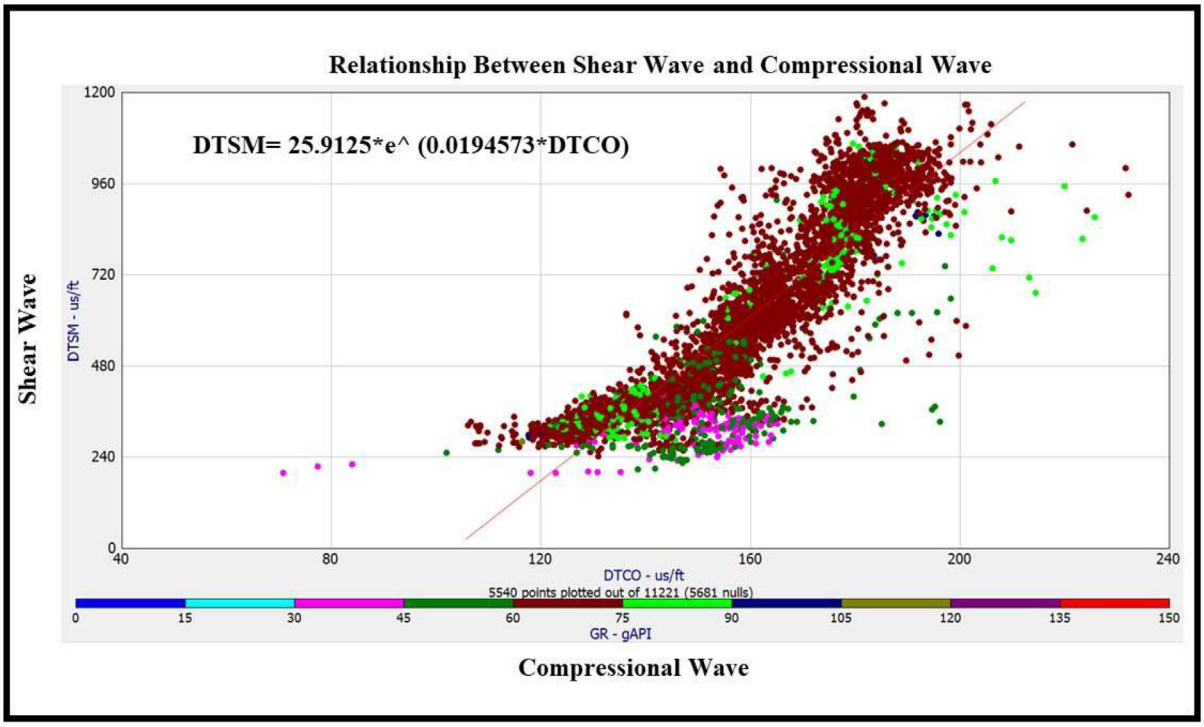

Fig. 10. Shear sonic vs. compressional sonic using GR values as discriminators.

inquiry into the Sapphire-Db Well (Fig. 10). The following equation can be used in the absence of shear sonic, which is crucial in all rock mechanics dynamic calculations:

$$DTSM = 25.9125 * e\hat{}(0.0194573 * DTCO)$$

6. Conclusion

Based on the findings presented in the previous section, several conclusions can be drawn. First, the geomechanical data obtained is valuable for constructing a one-dimensional mechanical earth model, particularly for predicting wellbore stability and establishing a safe mud window. In addition, empirical equations applied to compression sonic logs, shear sonic logs, and density logs allowed for the calculation of elastic properties. Moreover, a strong linear relationship between the elastic moduli and S-wave velocity in Sapphire sediments was observed, with a high correlation coefficient ($R^2 = 0.94$). Furthermore, regression analysis yielded an equation describing the relationship between compressional and shear velocities, which can be useful in cases where shear-wave data is absent. Variability in Poisson's ratio was noted, with shale zones exhibiting a wide range of values (0.41–0.48) and sandstone intervals demonstrating lower values (0.24–0.31), while siltstone values fell between those of sandstones and shale. Moreover, unconfined compressive rock strength predictions showed low values in sandstone but higher values in short intervals. An inverse relationship between total porosity and internal friction angle was observed, with effective porosity positively correlated with friction angle, particularly when shale volume decreased. Moreover, the results suggest that shale beds are more likely to experience instability issues due to their elevated Poisson's ratio and lower Young's modulus compared with other formations. Lastly, despite these findings, there are concerns about data reliability, primarily due to the absence of core findings, which could further validate the results.

Conflicts of interest

There are no conflicts of interest.

Acknowledgements

The authors extend their appreciation to the Egyptian General Petroleum Corporation (EGPC) and the Rashpetco Company management for their help in gaining publication approval for this study and giving access to the relevant data.

References

[1] Zhao Y, Feng Z, Xi B, Wan Z, Yang D, Liang W. Deformation and instability failure of borehole at high temperature and high pressure in hot dry rock exploitation. Renew Energy 2015;77:159–65.

[2] Fjar E, Holt R, Raaen A, Risnes R, Horsrud P. Petroleum Related Rock Mechanics: Mechanical properties and in situ stresses from field data. 2nd ed vol. 53; 2008. p. 391.

[3] Chang C, Zoback MD, Khaksar A. Empirical relations between rock strength and physical properties in sedimentary rocks. J Pet Sci Eng 2006;51:223–37.

[4] Higgins-Borchardt S, Sitchler J, Bratton T. Geomechanics for unconventional reservoirs. Unconvent Oil Gas Res Handbook 2016:199–213.

[5] Aal A, El-Barkooky A, Gerrits M, Meyer H-J, Schwander M, Zaki HH. Tectonic evolution of the Eastern Mediterranean Basin and its significance for hydrocarbon prospectivity in ultradeep water of the Nile Delta. Lead Edge 2000 Oct 1;19: 1086–102.

[6] Badawy A. Present-day seismicity, stress field and crustal deformation of Egypt. J Seismol 2005;9:267–76.

[7] Rio D, Sprovieri R, Thunell R. Pliocene-lower Pleistocene chronostratigraphy: a re-evaluation of Mediterranean type sections. Geol Soc Am Bull 1991;103:49–58.

[8] Donoso HG. Sensitivity analysis of geomechanical parameters in a two-way coupling reservoir simulation. Missouri University of Science and Technology; 2016. p. 15–7. Masters Theses. Paper 7596.

[9] Lucier A, Zoback MD, Gupta N, Ramakrishnan TS. Geomechanical aspects of CO2 sequestration in a deep saline reservoir in the Ohio River Valley region. Environ Geosci 2006;13:85–103.

[10] Xu S. In situ stress prediction from ductile deformation of unconventional reservoir rocks and its relation to the stress dependence of permeability. Stanford, California: Stanford University; 2020.

[11] Mavko G, Mukerji T, Dvorkin J. The rock physics handbook. 2009.

[12] Rajput S, Thakur NK. Tectonics and gas hydrates. In: Geol controls gas hydrate form unconvent; 2016. p. 107–30.

[13] Zoback MD. Reservoir geomechanics. Cambridge: Cambridge University Press; 2010.

[14] Zoback MD. Reservoir geomechanics: earth stress and rock mechanics applied to exploration, production and wellbore stability. 2007. p. 450.

[15] Lal M, Onyia EC, Kristiansen T, Walsgrove T, Bowers G, et al. Amoco Wellbore Stability Drilling Handbook. 1991.

[16] Jaeger JC, Cook NG. Fundamentals of rock mechanics. 3rd ed. Geol Mag 1980;117:401. 401

[17] Khaksar A, Taylor PG, Fang Z, Kayes T, Salazar A, Rahman K. Rock Strength from Core and Logs, Where We Stand and Ways to Go; 2009.

[18] Heidarian M, Jalalifar H, Rafati A. Prediction of rock strength parameters for an Iranian oil field using neuro-fuzzy method. J Artif Intell Data Mining 2016;4:229–34.

[19] Shahoo M, Ali M, Reza GR, Raoof G, Farhad S. Prediction of shear wave velocity using empirical correlations and artificial intelligence methods. NRIAG J Astronomy Geophys 2014;3: 70–81.

[20] Rasouli V, Pallikathekathil ZJ, Mawuli E. The influence of perturbed stresses near faults on drilling strategy: a case study in Blacktip field, North Australia. J Petrol Sci Eng 2011; 76:37–50.

[21] Lal M. Shale stability: drilling fluid interaction and shale strength. In: SPE Latin American and Caribbean Conference; 1999.

[22] McPhee CA, Lemanczyk ZR, Helderle P, Thatchaichawalit D, Gongsakdi N. Sand management in Bongkot Field, Gulf of Thailand: an integrated approach. 2000. SPE 64467.

[23] Plumb R. Influence of composition and texture on the failure properties of clastic rocks. 1994. SPE 28022.

[24] Weingarten JS, Perkins TK. Prediction of sand production in gas wells: Methods and Gulf of Mexico case studies. J Petrol Technol 1995;47(7):596–600.

[25] Perkins TK, Weingarten JS. Stability and failure of spherical cavities in unconsolidated sand and weakly consolidated rock. 1988. SPE 18244.